Suggested Citation

M. Gulzar, H.H. Masjuki, M. Varman M.A. Kalam, NWM Zulkifli, R.A Mufti, A.M. Liaquat, Rehan Zahid and A. Arslan "Effects of biodiesel blends on lubricating oil degradation and piston assembly energy losses" Energy 111 (2016): 713 –721.

Effects of biodiesel blends on lubricating oil degradation and piston assembly energy losses

M. Gulzar[a,b*], H.H Masjuki[a*], M. Varman[a], M.A Kalam[a], NWM Zulkifli[a], R.A. Mufti[b], A.M. Liaquat[c], Rehan Zahid[a,b], A. Arslan[a]

[a]Centre for Energy Sciences, Department of Mechanical Engineering, Faculty of Engineering, University of Malaya, 50603 Kuala Lumpur, Malaysia.

[b]National University of Sciences and Technology, NUST, Islamabad-44000, Pakistan.

[c]Department of Mechanical Engineering, Quaid-e-Awam University of Engineering Science & Technology, Nawabshah, Pakistan.

[*]Corresponding author. Tel.: +60 3 79674448; Fax: +60 379675317.

E-mail: mubashir_nustian@hotmail.com

[*]Corresponding author. Tel.: +60 3 7967 5245; Fax: +60 379675317.

E-mail: masjuki@um.edu.my

Abstract

Fuel is considered a major influencing parameter for engine oil condition during extended engine operation. Its effects on engine oil performance is required to be investigated with the implementation of the worldwide biodiesel mandate in various countries. This research monitored the influence of biodiesel on the condition of engine lube oil by long duration testing on three fuels: DF as the baseline; 20% palm biodiesel and 80% DF (PB20); and 20% jatropha biodiesel and 80% DF (JB20). The tests were carried out on a single-cylinder CI engine. Sump oil samples were collected at regular intervals during 200-hour tests, after which the rheological, tribological, and chemical properties of the samples were investigated. Results showed that the B20 fuels decreased the viscosity and increased the acidity of the engine oil. Piston ring-cylinder and piston skirt-cylinder tests, in which a high-stroke reciprocating test rig was used, showed a slight increase in friction and wear losses near the intervals of oil draining for the B20 fuels. Chemical analysis by Fourier transform infrared spectroscopy and ASTM standard testing showed a decrease in soot loading but an increase in the fuel residue, corrosiveness, and oxidation of the engine oil samples for B20 fuelled engine tests.

Keywords: Oil degradation, palm biodiesel, jatropha biodiesel , piston, endurance testing, wear loss

1. Introduction

Amidst concerns over energy security, environmental legislation, and increasing costs of fossil fuels, many countries are taking action to promote the use of biodiesel [1]. The implementation of the biofuel mandate in different countries has reduced dependence on fossil fuels, mitigated climate change, and created demand for domestic feedstocks as energy

sources. Around the world, 419.2 thousand barrels of biodiesel are being consumed each day. The two largest biodiesel consumers are the European Union and the United States, accounting for 218.4 and 60 thousand barrels per day, respectively [2]. The sharply growing global trend of biodiesel consumption is illustrated in **Fig. 1.**

Biodiesel is composed of fatty acid methyl esters (FAME), synthesized by the transesterification of crude vegetable oils and animal oil/fats. Common biodiesel feedstocks include corn and soy oil (US), rapeseed oil (Europe), and palm and jatropha oil (Southeast Asia). The physicochemical properties of biodiesel depend on feedstock and reaction kinetics, and its characteristics significantly differ from those of petroleum diesel. These features raise concerns over the effects of biodiesel on the lubricity and quality of engine oil. Related risks include excessive fuel residue, increased acidity, oxidation, soot loading, corrosiveness, and increased wear loss [3-5]. Diesel fuel (DF) can accumulate in lubricating oil, particularly in vehicles equipped with diesel particulate filters (DPFs). Biodiesel accumulates to a greater extent than diesel fuel because of its high boiling temperature; this accumulation means that biodiesel can remain in an engine oil sump for long periods [1]. Additionally, the esters in FAME are hydrolyzed, thus resulting in high concentrations of weak acids in lubricants [4]. Such phenomena decrease oil drain intervals and promote engine wear and corrosion. High rate of lubricant degradation accounts for a major proportion of the million tons of annually produced oil wastes, which are hazardous and non-biodegradable [6]. Given that different studies highlight the effects of biodiesel on engine oil performance, automobile companies have cautiously recommended the use of biodiesel blends, allowing a maximum of 20% biodiesel (B20) to be blended with fuels for certain vehicles [1]. The ACEA European specifications for diesel engine oils require the implementation of OM646LA [7] and OM501LA [8] engine tests to ascertain the ability of biodiesel to preserve the performance of lubricating oil. Few studies have been devoted to the impact of biodiesel on lubricating oil

performance under extended engine operation. Previous investigations involved endurance engine testing, in which degraded oil samples were collected, and DF, ultra-low-sulfur diesel (ULSD), and a few biodiesel feedstocks were analyzed. The extensively used feedstocks in previous research include rapeseed, soybean, and linseed biodiesels [1, 9-12]. The general conclusions presented in the literature are consistent with one other; specifically, these indicate that high biodiesel blends increase fuel residue [13], accelerate engine oil degradation [4] [14], and increase corrosion [4] [14]. These key findings underscore the need to reduce the oil drain intervals for vehicles running on blends that comprise a biodiesel content of more than 5% (B5). No significant difference in soot loading and engine wear has been found between vehicles using ULSD and specific biodiesels [1] [4, 15].

One of the major factors that drive variations in engine oil condition is the change in biodiesel feedstocks. With the emergence of a variety of feedstocks for biodiesel production, the influence of biodiesel fuel manufactured from these raw materials requires investigation, specifically in relation to engine oil performance under extended engine operation. This study aspires to fill this need by conducting 200 hours of engine tests on two biodiesel blends: 20% palm biodiesel and 80% DF (PB20) and 20% jatropha biodiesel and 80% DF (JB20). The tests were carried out on a single-cylinder diesel engine. For comparison, engine test was also performed on the DF under the same testing conditions as those applied in the tests on the B20 fuels. For each test, several engine oil samples were collected to analyze oil degradation. Oil analysis comprised three stages: (1) rheological analysis of oil physical characteristics by ASTM standard testing; (2) chemical analysis by Fourier transform infrared (FTIR) spectroscopy and ASTM standard testing; and (3) tribological analysis for the laboratory-based friction and wear testing of the piston ring–cylinder and piston skirt–cylinder interactions.

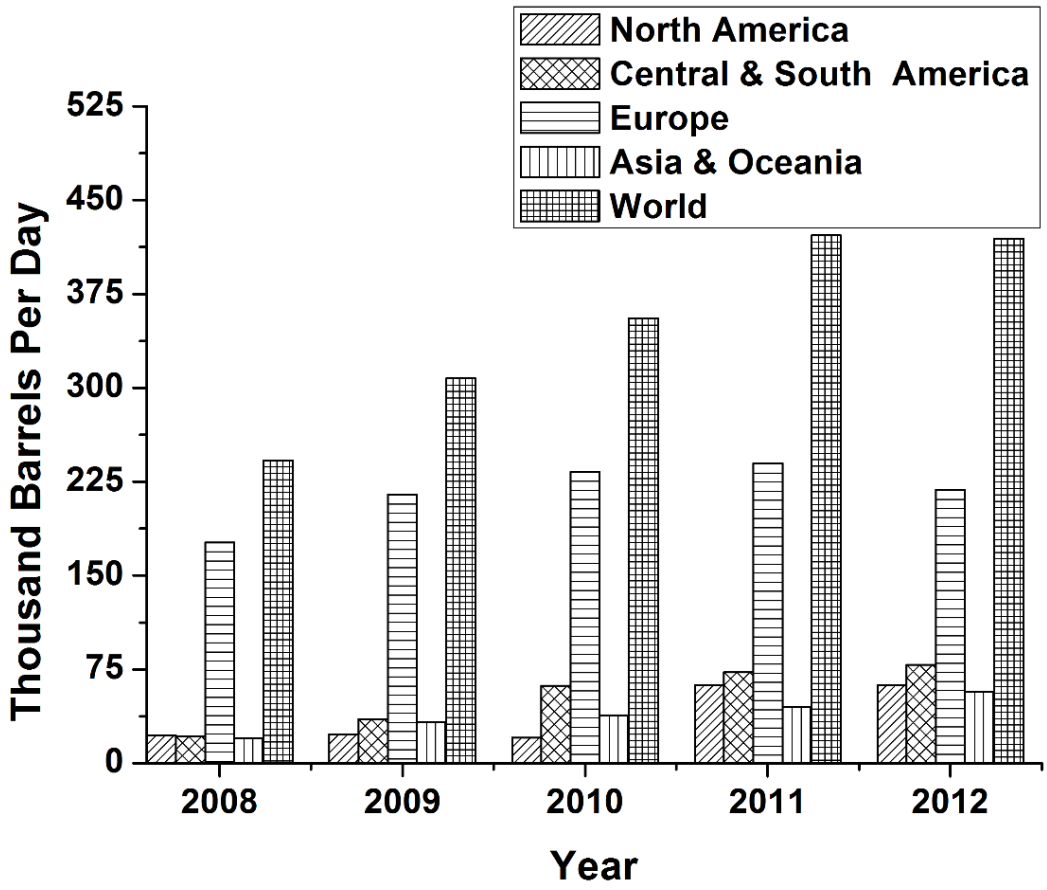

Fig. 1 Trend of regional yearly biodiesel consumption [2]

2. Materials and methods

A naturally aspirated, single-cylinder diesel engine was used in the experiments. The engine specifications for relevant parameters are given in **Table 1**. Engine testing was performed on three different fuels which include diesel fuel (DF), 20% palm biodiesel and 80% DF (PB20); and 20% jatropha biodiesel and 80% DF (JB20). For the DF and B20 fuels, the necessary fuel properties were measured on the basis of ASTM standards (**Table 2**). A fully formulated lubricant, 15W40, which conforms to API specification CJ-4, was employed

in the endurance tests. **Table 3** provides the technical specifications of the engine oil used in this study.

Table 1. Relevant engine specifications.

Parameter	Specification
Model	YANMAR TF 120-M
Configuration	Single cylinder
Air aspiration	Naturally aspirated
Maximum Power	7.7 kW
Maximum Speed	2400 rpm
Fuel injection	Mechanical direct injection
Displacement	0.638 L
Oil capacity	2.8 L
Oil change interval	200 hours

2.1 Engine oil sampling

To evaluate the effects of each of the fuels on lubricant degradation, the single-cylinder diesel engine was tested at 10-Nm loading and 2000 rpm for 200 hours. The engine was coupled to an eddy current dynamometer and data acquisition system. The schematic of the experimental setup is shown in **Fig. 2.** The Dynomax 2000 software was used to operate the engine at the required test conditions. Engine maintenance was conducted and oil samples were collected at regular intervals of 40 hours. At each interval, the minimum volume required for the oil analysis was extracted to reduce the amount of fresh makeup oil for maintaining the oil level.

Table 2. Properties of diesel fuel and bio-diesels.

Properties	ASTM test standard	Test Equipment	Manufacturer	DF	PB20	JB20	ASTM limits for biodiesel
Kinematic viscosity at 40°C (cSt)	D 7042	SVM 3000	Anton Paar, UK	3.317	3.62	3.53	1.9-6.0
Flash point (°C)	D 93	Pensky-martens NPM 440	Normalab, France	69	89	74	130
Density at 15°C (kg/m^3)	D 7042	SVM 3000	Anton Paar, UK	822	833	834	N/S
Calorific value (MJ/kg)	D240	C2000 basic calorimeter	IKA, Germany	45.55	43.83	43.74	N/S
Cetane number	D6890	Advanced engine technology IQT™		51	53.1	51.9	

Table 3. Typical engine oil characteristics

SAE 15W40	Viscosity at 100 ^0C	16.1 (cSt)
	Density at 15 ^0C	0.865 (g/cm^3)
	TBN	10

	(mgKOH/g)		
		Sulfated Ash	1%

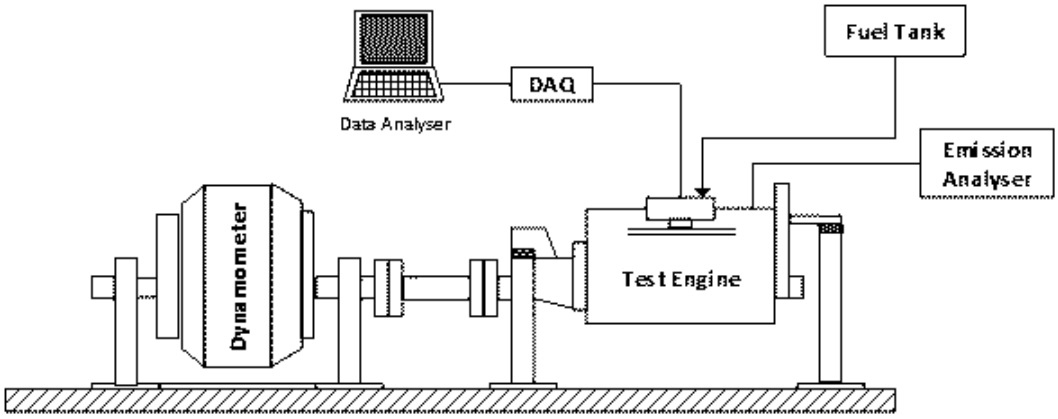

Fig. 2 Schematics of the engine test bench.

2.2 Rheological analysis

In the rheological analysis, engine oil viscosity, density, and acidity were examined by adopting ASTM standard testing procedures. The kinematic viscosity and density was measured using ASTM D7042 standard. In this study, calorimetric titration was used to examine the TAN characteristics of new and degraded oil samples, in accordance with the ASTM D664 standard. An alcoholic solution of KOH was used to neutralize 2 g of each sample oil and the TAN values are reported in mgKOH/g of oil.

2.3. ***Chemical Analysis***

For chemical analysis of oil samples, FTIR spectroscopy was used to investigate the fuel residue, oxidation, and soot loading while corrosion resistance was analyzed using ASTM standard testing.

2.3.1 FTIR spectroscopy

The lubricant samples were analyzed by FTIR spectroscopy for fuel residue, oxidation, and soot loading. These parameters were evaluated with a PerkinElmer Spectrum 400 FTIR spectroscopy instrument with a data acquisition system. A background spectrum was obtained as reference before FTIR measurements were conducted. It was ensured that the crystal surface was clean and properly installed before the background spectrum was obtained. For FTIR analysis 21 oil samples were used. These samples include 18 engine sump oil samples collected at six regular intervals for three endurance tests. In addition, 3 fresh lubricant samples were used to get the reference background for oil analysis tested by each fuel. The spectra were acquired over a spectral range of 4000–500 cm^{-1} at 2 cm^{-1} spectral resolution; 16 scans per test were selected. The absorbance spectra mode was chosen for data analysis. The monitoring parameters for lubricant oil condition and reporting methods (range of wavenumber) are listed in **Table 4.**

Table 4 – Lubricant condition monitoring parameters and reporting using FTIR

Parameter	Measurement Region (cm^{-1})	Baseline Point(s) (cm^{-1})	Reporting*	Interferences	Type of Measurement	Relative Sensitivity
Diesel	815 to 805	Minima 835 to 825 and 805 to 795	(Value + 2) × 100	Fuel evaporation, variation in fuel aromaticity	Contaminant screening	extremely sensitive
Oxidation	1800 to 1670	Minima 2200 to 1900 and 650 to 550	Report Value as Measured	Dispersants, moisture contents, VI improvers	Trending lubricants degradation	fairly insensitive
Soot Loading	2000	None	Value × 100	Particle size, particle density, engine make/model	Trending carbon load for diesel engine	insensitive

* Reporting values in absorbance/0.1mm

2.3.2 Corrosiveness

The corrosion of aluminum alloy Al5083 immersed in degraded oil samples was investigated in accordance with the ASTM D4636 standard test on lubricant corrosiveness. Square aluminum specimens with a length of 20 mm and a thickness of 5 mm were used. Prior to the corrosion test, the specimens were polished to remove the oxide layer and washed in acetone. Glass beakers containing the oil samples and Al5083 specimens were heated at a constant temperature of 135 °C for 168 hours while air was blown toward the oils to induce agitation and provide oxygen supply. To further investigate the surface morphology of the immersed aluminum specimens, SEM micrographs and EDX were taken. The surface characteristics of the corroded surface were analyzed using a Phenom ProX scanning electron microscope at an electron-accelerating voltage of 15 kV. EDX spectrum was used to identify the elements existing on the selected wear scar surfaces. To quantify the corrosion resistance of the lubricant samples, the corroded aluminum specimens were polished by using silicon carbide paper. The specimens were then washed in acetone and dried. The weight loss of each specimen was calculated on the basis of its weight prior to and after the immersion test by using a weighing balance with an accuracy of 0.1 mg. The data obtained from the weight loss measurements were converted into corrosion rates (µm/y) by

$$\text{Corrosion rate} = \frac{8.78 \times 10^{9} w}{DtA}$$

(1)

where “w” is the weight loss (kg), “D” denotes the density (kg/m^3), “A” represents the exposed surface area (m^2), and “t” is the exposure time (h).

2.4. Tribological Analysis

To simulate actual engine conditions, specimens were extracted from the piston ring, piston, and cylinder liner of a commercial diesel engine. A CNC wire-cut EDM was used to machine

the samples and prevent damage to surface treatments. A high-stroke reciprocating test rig was used, so that the piston ring/piston skirt holder was stationary at the top and that the specimen of the cylinder liner moved in a reciprocating motion. The specimen taken from the cylinder liner was placed in a lubricant bath, where the oil temperature was regulated using a control panel. After load application, conformal contact between the reciprocating surfaces was established. To simulate engine oil temperature, the oil bath was equipped with a temperature controller, a thermocouple, and a heater system. Friction and wear properties were measured using the test conditions indicated in **Table 5**. The considered loading conditions were used to simulate a maximum engine speed of 1.1 m/s and a contact pressure of ~10 MPa, following the test conditions stated by Gullac and Akalin [16]. The experimental setup is illustrated in **Fig. 3**. The data acquisition system attached to the test rig provided the friction data, whereas the weight loss method provided the wear measurements. For each test, the specimens were ultrasonically cleaned and weighed to an accuracy of 0.1 mg. Running in duration lasted for two hours; thus, rough edges on new surfaces were shaved off before each test.

Table 5 Test conditions for high stroke reciprocating test rig.

Normal load	160 N
Temperature	70 °C
Stroke	84 mm
Contact width	25.4 mm
Speed	240 rpm
Lubricant feed rate	5 mL/hr

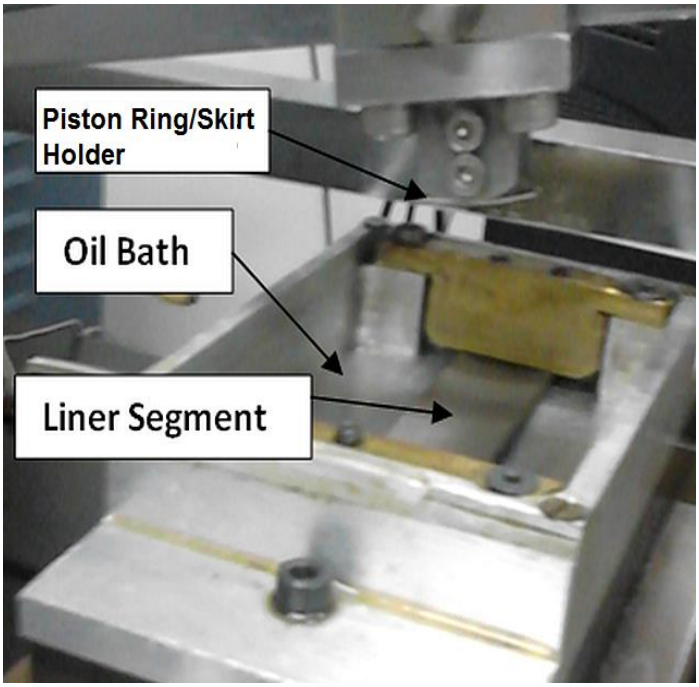

Fig. 3 Piston ring/skirt and liner experimental setup in reciprocating test rig

3. Results and discussion

The oil samples were analyzed using standardized methods in order to determine the lubricant's rheological, chemical and tribological characteristics. To assess the true condition of the oil, the findings of all of the features of each sample were considered and compared with baseline.

3.1 Rheological characteristics

3.1.1. Viscosity

Engine oil viscosity is one of the key physical parameters for assessing oil condition during endurance testing. For badly degraded oil, sludge and soot particles rapidly increase viscosity under extended engine operation. In this study, no increase in viscosity was observed for any of the fuels. Instead, engine oil viscosity gradually decreased over time. **Fig. 4** illustrates the

trend with which the kinematic viscosity changed during the course of the endurance tests on all the fuels. To compare the viscosity trends with previous studies related to engine endurance testing [1, 17-19], viscosity results at 100 ^{o}C are reported. The researchers have mentioned that 100 ^{o}C is close to the average engine operating temperature [20, 21]. The trend of viscosity results shows that after an initial oil thinning at 40 hrs, insignificant variation in engine oil viscosity has been observed for 80 hrs sample. This was due to an average oil sump temperature of 93 ^{o}C at 80 hrs which shows the tendency of all fuels residues to evaporate from the oil sump. Later on, the share of polymers used as viscosity modifiers was likely to cause oil thinning over long hours operations [17]. The kinematic viscosities dropped to as low as 10.7 and 11.1 cSt in the engine tests featuring the B20 fuels and DF, respectively. This trend can most likely be attributed to the higher fuel residue caused by the B20 fuels. Zdrodowski et al. [1] also reported a reduction in the engine viscosity of B20-fuelled vehicles compared with ULSD-fuelled vehicles for which engine oil samples were collected over long mileage. For 15W-40 engine oil, viscosity was dropped to 10.7 and 10.74 for PB20 and JB20 respectively. The reduction rate of oil viscosity was low for PB20- and JB20-fuelled engines as compared to B20 counterparts. Zdrodowski et al. [1] reported kinematic viscosity as low as 6.6 cSt for engine running on B20 fuels when 15W-40 engine oil was used. Similarly, Stepien et al. [17] reported that, for heavy duty engine testing, the engine oil viscosity decreased significantly with rapeseed biodiesel. Therefore, the use of B20 fuels results in oil thinning over the long hour test duration which in turn reduce the lubricant film thickness between engine interacting parts.

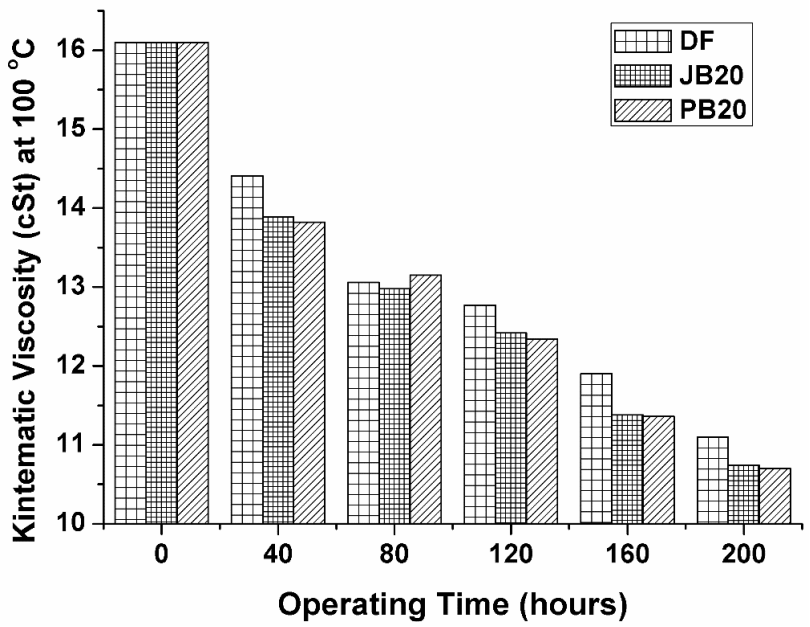

Fig. 4 Kinematic viscosity at 100 ^{o}C vs engine operating time.

3.1.2 Density

The analysis of engine oil density indicates the degree of contamination by wear metals and fuel residue. An increase in oil density represents substantial contamination by wear debris, fuel residue, and increased moisture content [22]. In the endurance tests on the B20 fuels, fuel residue reduced the lubricant film thickness between interacting engine parts, thus promoting wear of engine components. **Fig. 5** shows the changes in the engine oil densities of the oil samples collected at regular intervals during endurance testing. Because of the combined effects of wear debris and fuel residue, engine oil density increased to a greater extent when the B20 fuels were used than when the DF was used. For all the lubricant samples, PB20 exhibited the highest density. The maximum increases in oil density were 0.895 g/cm^3 for DF, 0.901 g/cm^3 for JB20, and 0.903 g/cm^3 for PB20. Liaquat et al. reported similar trends for DF, PB20, and JB20 under extended engine operation [23, 24].

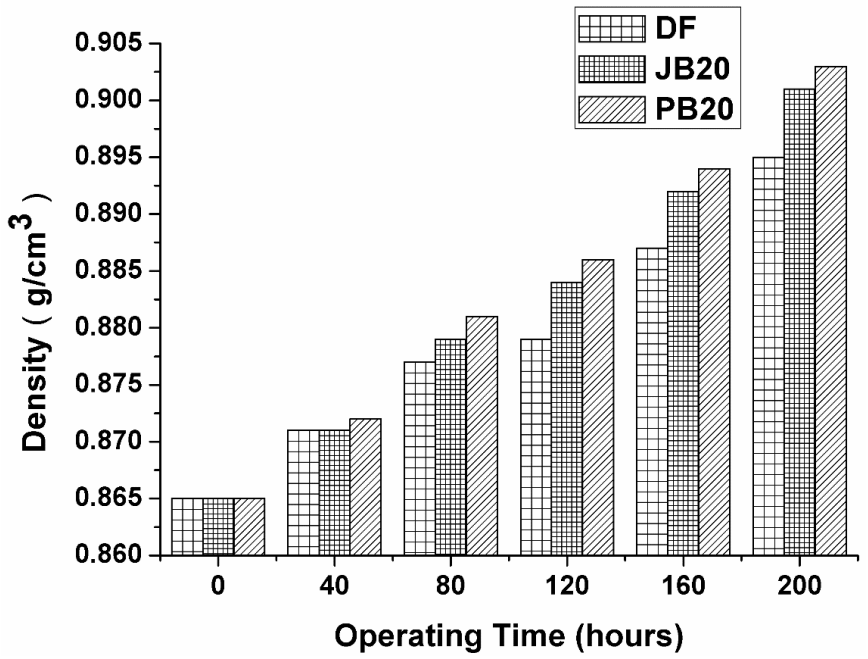

Fig. 5 Density at 15 ^{o}C vs engine operating time

3.1.3. Acidity

Lubricant acidity is regarded as the primary indicator of an engine's oil drain interval and is commonly measured as the total acid number (TAN). In engine operation, TAN typically increases over time, yet an essential requirement for preventing corrosion and oxidation is the low acidity of engine oil [25]. **Fig. 6** indicates the TAN values of the oil samples taken after regular intervals of 40 hours. With either the DF or B20 fuels, the TAN values ranged from 1.87 to 2.5 mg KOH/g oil for the new and aged oils, respectively. With the B20 fuels, the TAN values slightly changed. The TAN values of the B20 fuel were low for the first 80 hours of engine operation and increased after 120 hours. This result may be related to the time that elapsed before the B20-fuelled engine hydrolyzed the esters in the sump; the hydrolyzation produced additional weak organic acids, thereby suddenly increasing the TAN values [26]. The higher rate of acidity in oil samples tested with B20 show low alkaline reserve in the lubricant samples which corresponds to short useful life of lubricant than that of DF.

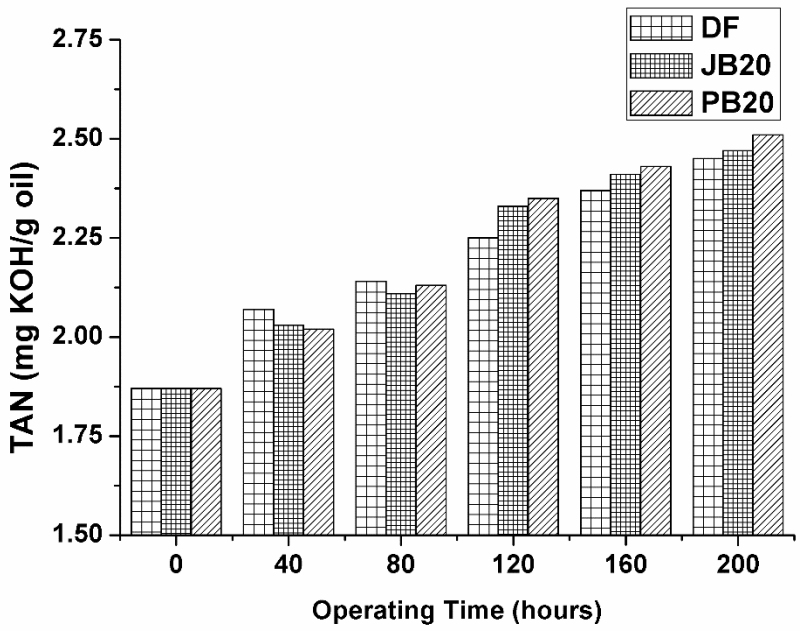

Fig. 6 TAN vs engine operating time

3.2 Chemical Characteristics

During FTIR analysis, for baseline characteristics, fresh lubricant was scanned, and relevant spectrum values were used to derive the corrected absorption values of each parameter considered for the used oil samples.

3.2.1 Fuel residue

Detecting fuel residue in engine oil by any method is difficult because fuel and base oil differ in terms of molecular weight, boiling temperature range, and aromatic compound content. The IR absorption method enables the examination of the aromatic compounds in engine oil, and thereby, the determination of fuel residue. The difference in aromatic compound content between engine oil and fuel reflects fuel residue. In this work, therefore, the spectra of the fresh engine oil around 800 cm^{-1} was taken as the baseline for detecting possible fuel residue. The absorption intensity of the fresh engine oil was measured, and the change in its absorption spectrum was determined as it was being diluted. The IR absorption value of each absorbance spectrum was derived for all the collected samples and plotted for comparative

analysis. **Fig. 7** shows the fuel residue in the used engine oil samples. During the initial hours of engine testing, no significant change in fuel residue for all the fuels was observed. After 80 hours of engine testing, the fuel residue increased for the B20 fuels. The high fuel residue of the engine oils in the biodiesel-fueled engines is expected because biodiesels have a volatility lower than that of DF [27]. The fuel residue of the B20 fuels therefore remained in the oil sump and gradually evaporated at the related oil sump temperatures. Other factors that influence the production of fuel residue in engine oils include the fuel mass post-injected into cylinders and the frequency of DPF regeneration [1]. This tendency of high fuel residue during B20 fueled engine testing shows higher acidic contamination due to hydrolysis of esters in biodiesels. This acidic contamination results in higher rate degradation of engine lubricant. At the end of 200 hours' test, a fuel residue of 10.7% and 11.74% has been observed for engine oil conditioned with PB20 and JB20 fuels respectively. The fuel residue at the drain interval is low as compared to previously reported long duration engine testing, as in one of the study for 20% soybean biodiesel dilution, fuel residue of 35% was reported [1].

3.2.2 Oxidation

The IR-derived oxidation values were obtained from the spectrum peaks between 1800 to 1670 cm^{-1} **(Table 4).** The oxidation values at absorption mode were due to the absorption of IR energy by the carbon oxygen bonds in the degraded oil. Only a limited number of fresh petroleum oil compounds exhibited significant absorptions in the 1800–1670 cm^{-1} region. For the used oil, therefore, the spectral peaks in this region serve as a direct measurement of the oxidation level in the engine oil. For each oil sample, the highest IR absorption peak was determined on the basis of the above-mentioned wavenumber range. **Fig. 8** illustrates the oxidation levels of the analyzed lubricant samples. The increasing trend of oxidation was more noticeable in the B20 fuels than in the DF. Changes in feedstock and percentage dilution

of FAME affect the oxidation of used engine oils [1, 17]. The oxidation values of the DF were significantly low throughout the endurance tests. PB20 showed high oxidation values after the first few hours of testing. This result can be related to the depletion of antioxidants in the corresponding engine oil samples; the depletion is caused by high fuel residue and increased acidic contamination. Thus the use of biodiesel blends affects the lubricant additives concentration over the endurance testing which can result in short useful life of lubricant.

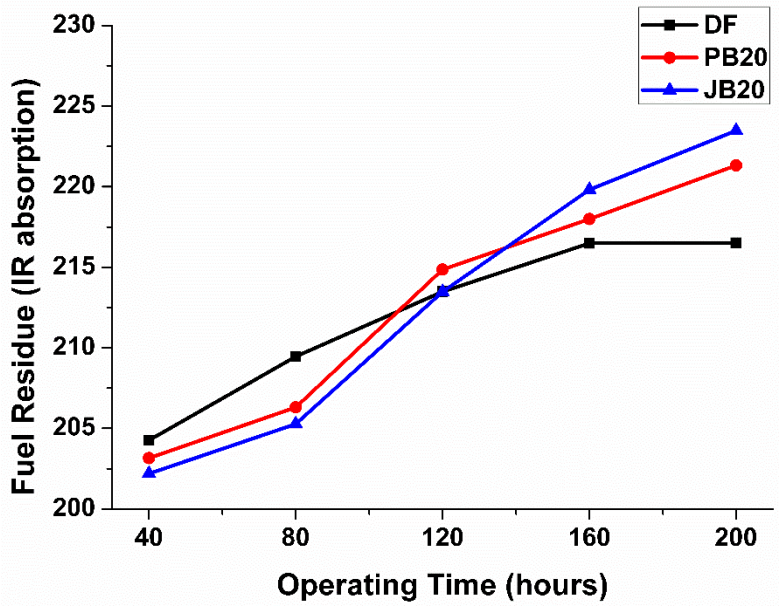

Fig. 7 FTIR fuel residue vs engine operating time

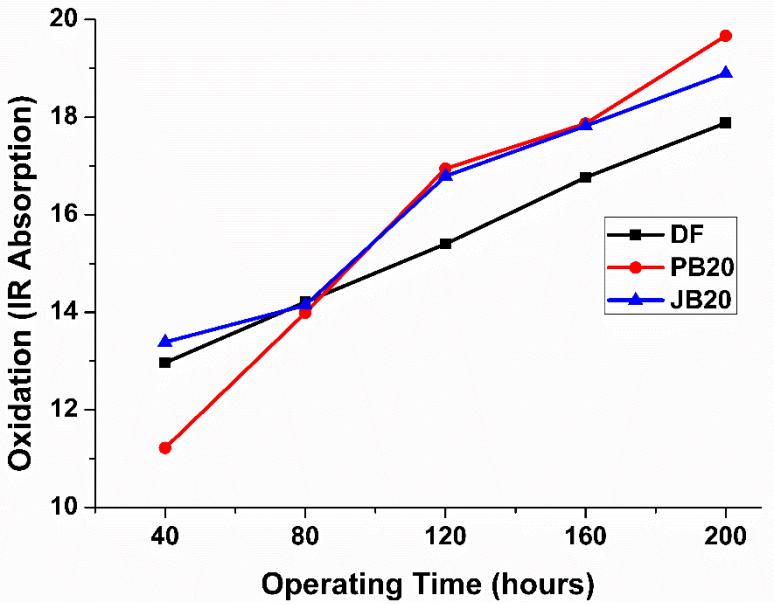

Fig. 8 FTIR oxidation vs engine operating time

3.2.3 Soot

The combustion of highly rich fuel/air mixtures produces soot and soot particles form as a result of incomplete fuel combustion. Petroleum diesel exhibits a high tendency toward soot formation because of its low H/C ratio, but diesel blends with high H/C contents can reduce the occurrence of this problem [28]. Soot formation in engine oils increases oil viscosity and prematurely blocks the oil filter and oil circuit. Although soot has no particular IR absorption bands in an FTIR spectrum, it causes a scattering of IR radiation, which tends to be severe at high wavenumbers. In this work, therefore, soot loading was considered the absorbance intensity value at 2000 cm^{-1}. In this study, the high soot content of the engine oil reflects combustion problems for extended drain intervals. **Fig. 9** indicates that soot content steadily increased throughout the endurance tests on all the cases. Given that biofuels help reduce particulate matter emissions and smoke opacity [29] [30, 31], the amount of soot produced by the samples collected from the oil sump also decreased near the intervals of oil draining. Accordingly, soot loading by FTIR absorbance spectra was lower for the B20 fuels than for

the DF. The results show that the considered B20 fuels are suitable to decrease the soot content which shows the related environmental advantage over DF.

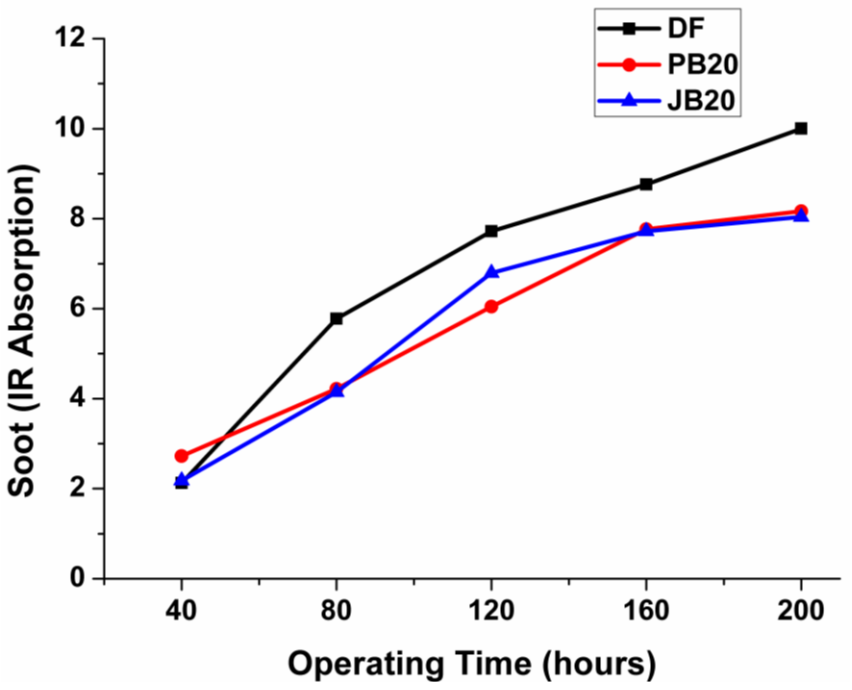

Fig. 9 FTIR soot loading vs engine operating time

3.2.4 Corrosiveness

Diesel dilution enhances material degradation and corrosion given that biodiesels are oxidative in nature; this property originates from the high concentrations of unsaturated molecules in biodiesels [32]. The corrosion rates of the aluminum specimens are shown in **Fig. 10.** For investigation of the surface morphology of immersed aluminium specimen, **Fig. 11** shows the SEM micrographs together with EDX. A number of small pits with noticeably different sizes and frequencies formed in a random manner on the surfaces of all the specimens (**Fig. 11**). The specimen immersed in the DF exhibited only a few small pits compared with the specimens immersed in PB20 and JB20. Numerous white small pits formed on the specimen immersed in JB20 (**Fig. 11(c))**. EDX analysis was conducted to

confirm the elemental composition of the small pits (**Fig. 11**). The elemental analysis of the surfaces where the small pits formed showed the presence of oxygen, even after specimen cleaning. The trend of the corrosion rate in **Fig. 10** agrees with the SEM/EDX results, as indicated by the highest corrosion rate generated by JB20. High corrosion rate shows that considered B20 fuel can cause corrosive attacks to engine metal parts during prolonged use. This behavior of B20 and higher blends can result in short life of engine parts.

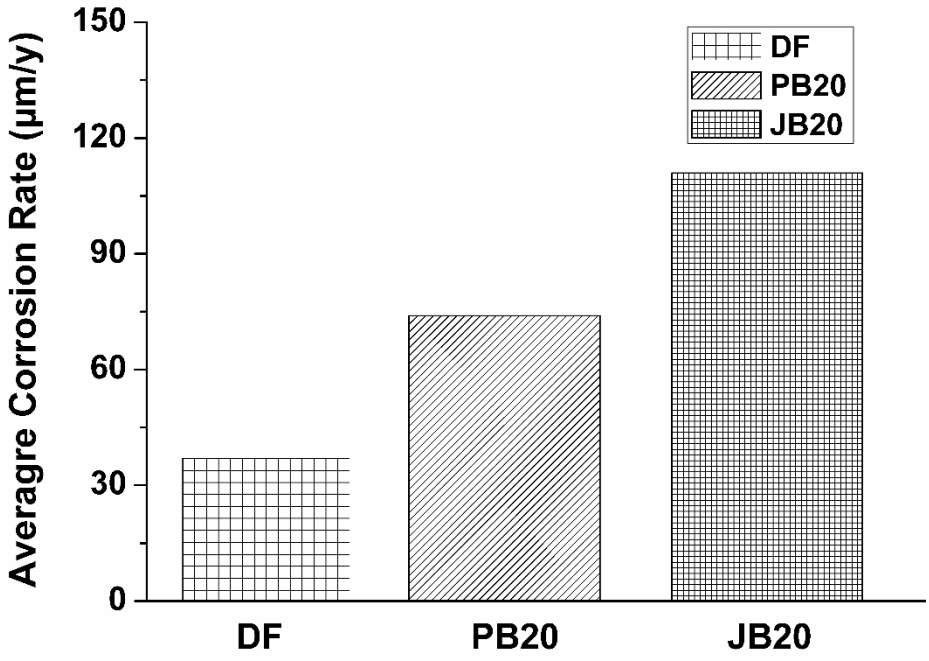

Fig. 10 Corrosion rate of aluminium in degraded lubricant samples.

Element	Conc. (Wt%)
Al	76.3
Fe	10.4
O	5.8

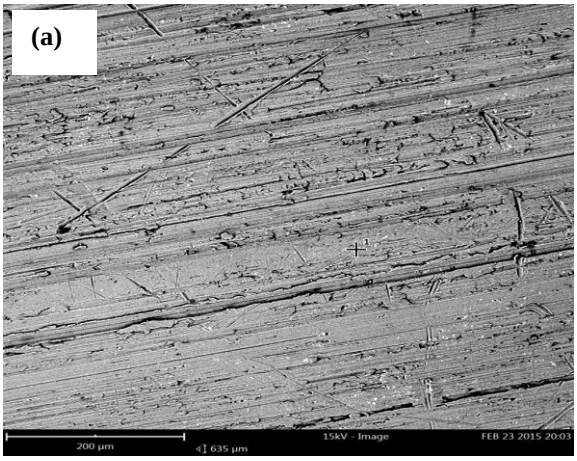

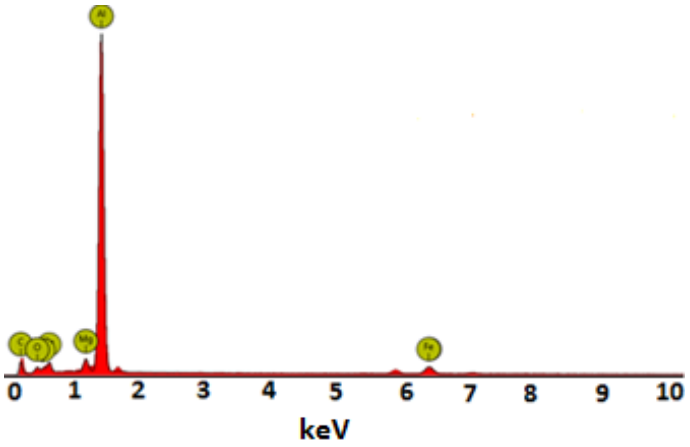

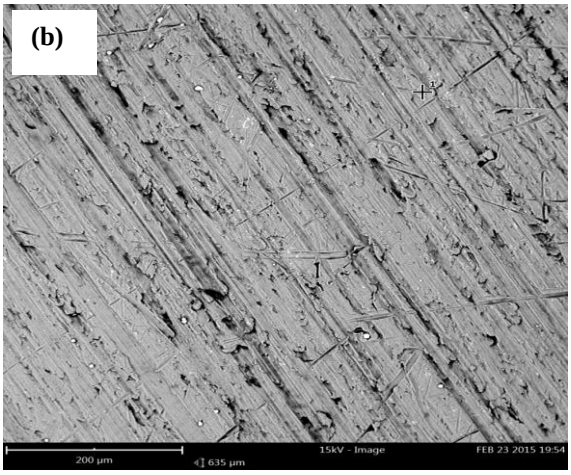

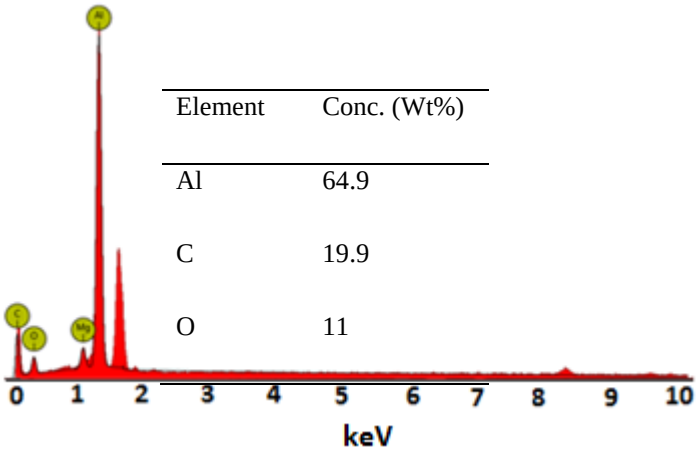

Element	Conc. (Wt%)
Al	64.9
C	19.9
O	11

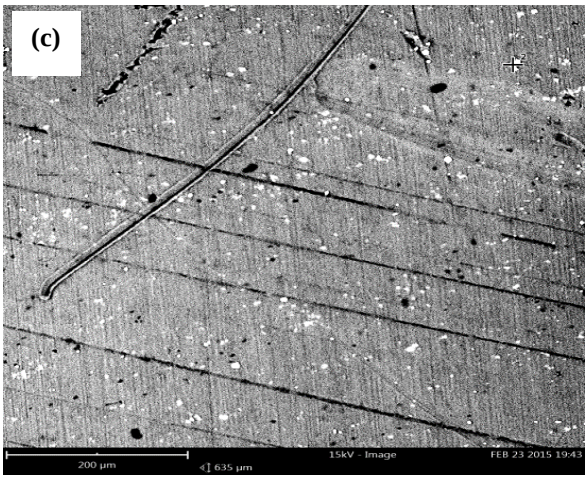

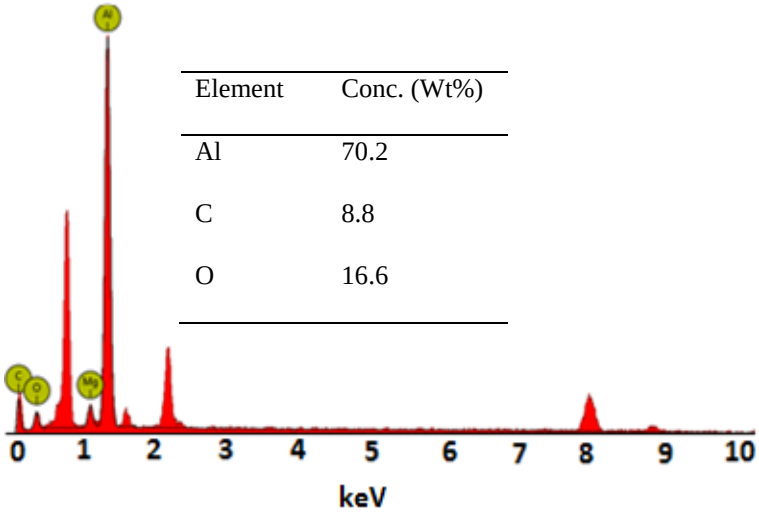

Element	Conc. (Wt%)
Al	70.2
C	8.8
O	16.6

Fig. 11 SEM and EDS graphs of metal surface after corrosion tests (a) DF (b) PB20 (c) JB20.

3.3 Tribological Characteristics

3.3.1 Friction

The oil characteristic that can be reasonably assumed to affect the friction coefficient is oil viscosity. The oil viscosity of the analyzed oil samples was directly influenced by fuel residue. Lubricant viscosity plays a critical role in lubricant film formation under hydrodynamic and, to some extent, mixed lubrication conditions, which manifest at a piston's mid-stroke position and in bearings. A high rate of fuel residue occurred in the engine oils collected from the B20-fuelled engine. This dilution caused low viscosity and ultimately reduced the thickness of the film separating the interacting surfaces. The mixed lubrication regime is expected under the simulated engine conditions. The lubricant viscosity effects on the friction coefficients of the piston ring–cylinder and piston skirt–cylinder interactions are depicted in **Figs. 12** and **13**, respectively. The figures indicate that initially, the variations in friction coefficient were insignificant for all the oil samples, but as fuel residue increased after 80 hours of testing, high friction coefficients occurred for the B20 fuels. These trends show that as the fuel residue increased in the oil sump, lubricant film thickness was reduced. The increasing friction behavior over the endurance tests for B20 fueled engine show the undesirable change in the concentration of friction reducing additive. The friction coefficient of the piston ring–cylinder interaction ranged from 0.095 to 0.167. The lowest and highest friction coefficients of the piston–skirt sliding were 0.119 and 0.175, respectively.

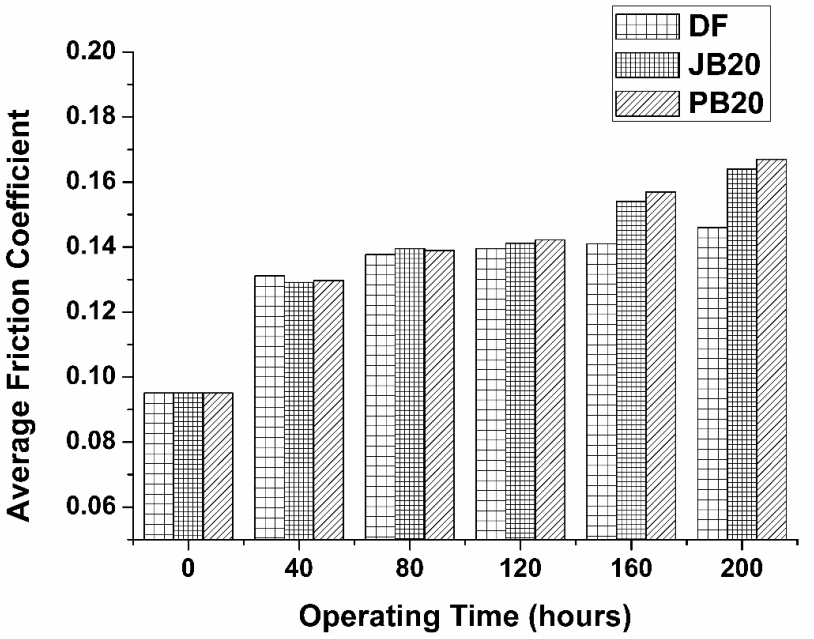

Fig. 12 Friction coefficient for piston ring-cylinder reciprocating test.

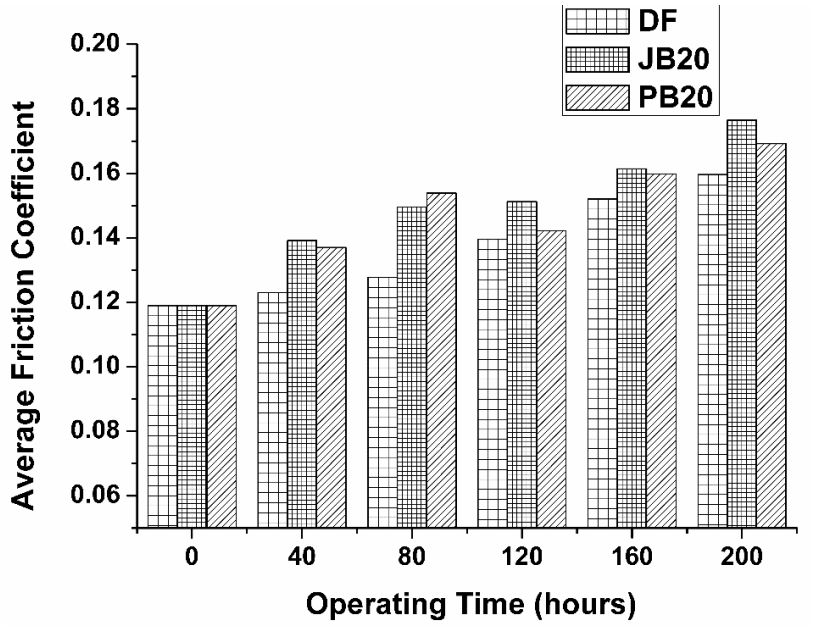

Fig. 13 Friction coefficient for piston skirt-cylinder reciprocating test.

3.3.2. Wear

Wear is expressed in terms of the weight loss of a cylinder liner specimen used in reciprocating wear tests. **Figs. 14-15** illustrate the wear of the cylinder liner for piston ring-cylinder and piston skirt-cylinder wear tests, respectively. The results are the average of at least two tests. The wear rate was similar across the evaluated cases. The lowest wear rate was

generated by the DF given that the related oil samples produced the highest viscosity and lowest fuel residue. For B20 fueled engine testing, increased fuel residue reduces lubricant viscosity, which facilitates the adhesive wear and lubricant additives depletion. The depleted additives include anti-wear compounds; thus, high fuel residue enhances wear rate. Furthermore, the active chemical characteristics of soot content badly affect the wear resistance of tribofilm-forming additives, such as zinc dialkyl dithiophosphate [33]. For the piston ring–cylinder interaction, the cylinder liner weight loss ranged from 1.2 to 5.8 mg. For the piston skirt–cylinder interaction, the weight loss due to wear ranged from 2.15 to 8.95 mg. The increased weight loss of the piston skirt specimen is due to the fact that the piston skirt was not coated and the specimen has a contact area larger than that achieved in the piston ring–cylinder interaction.

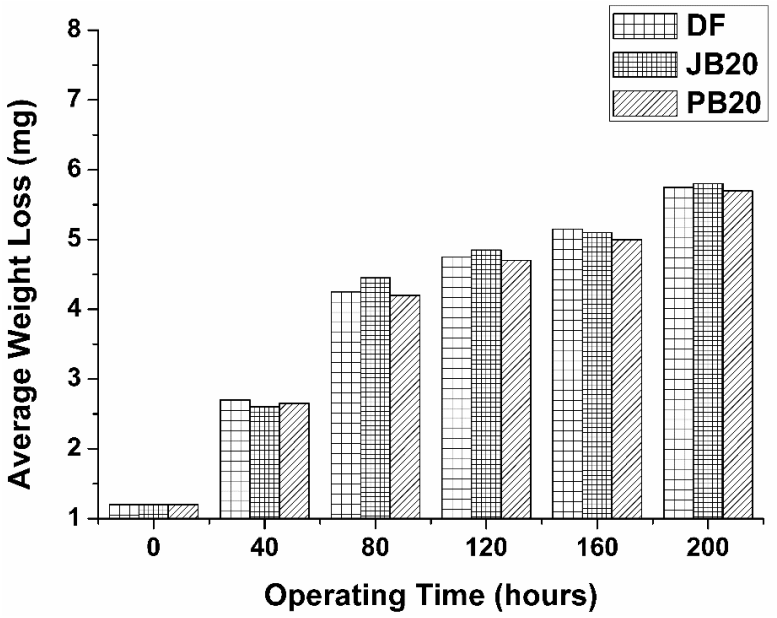

Fig. 14 Cylinder liner wear rate for piston ring-cylinder reciprocating test.

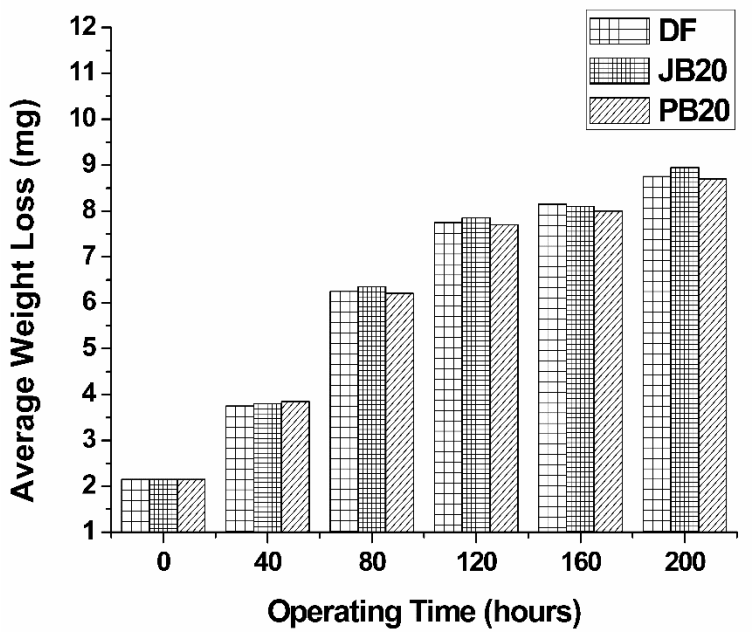

Fig. 15 Cylinder liner wear rate for piston skirt-cylinder reciprocating test.

4. Conclusion

This study investigated the effects of biodiesel blends on engine oil condition and lubricity. The key findings are summarized as follows:

- The B20 fuels increased fuel residue to an extent higher than that produced by DF, which reduced engine oil viscosity and increased oil acidity.
- FTIR analysis showed that the engine oils conditioned with B20 fuels produced significantly lower soot loadings than did DF.
- B20 fuels caused the accelerated depletion of additives in the engine oil as compared to DF.
- The laboratory high-stroke reciprocating tests showed slightly increased friction and wear with oil aging for the B20 fuels and DF.

- PB20 showed a lower engine oil degradation than that generated by B20 fuels made from other feedstocks.
- High corrosion rate and accelerated oxidation by B20 fuels showed that the considered biodiesel blends tend to reduce the lubricant useful life during the engine endurance tests.

Acknowledgements

The authors would like to thank the University of Malaya, which made this study possible through the High Impact Research Chancellory Grant, Project title: ‘‘Development of Alternative and Renewable Energy Carrier’’ Grant Number: UM.C/HIR/MOHE/ENG/60 and UMRG Grant RP016-2012A.

References

[1] R. Zdrodowski, A. Gangopadhyay, J.E. Anderson, W.C. Ruona, D. Uy, S.J. Simko. Effect of Biodiesel (B20) on Vehicle-Aged Engine Oil Properties. SAE Technical Paper. 2010-01-2103 (2010).
[2] EIA. International energy statistics. US Energy and Information Administration, Washington, DC, 2014.
[3] C. Rakopoulos, K. Antonopoulos, D. Rakopoulos, D. Hountalas, E. Giakoumis. Comparative performance and emissions study of a direct injection diesel engine using blends of diesel fuel with vegetable oils or bio-diesels of various origins. Energy Convers Manage. 47 (2006) 3272-87.
[4] C.C. Devlin, C. Passut, R. Campbell, T.-C. Jao. Biodiesel fuel effect on diesel engine lubrication. SAE Technical Paper. 2008-01-2375 (2008).
[5] H.L. Fang, S.D. Whitacre, E.S. Yamaguchi, M. Boons. Biodiesel impact on wear protection of engine oils. SAE Technical Paper. 2007-01-4141 (2007).
[6] M. Shahabuddin, H. Masjuki, M. Kalam, M. Bhuiya, H. Mehat. Comparative tribological investigation of bio-lubricant formulated from a non-edible oil source (Jatropha oil). Ind Crops Prod. 47 (2013) 323-30.
[7] K. Daniel, P. Kunz. CEC-L-99-08, Evaluation of Engine Crankcase Lubricants. Encyclopedia of Lubricants and Lubrication. (2014) 221-5.
[8] K. Daniel, P. Kunz. CEC-L-101-09 Heavy Duty Diesel Engine Test. Encyclopedia of Lubricants and Lubrication. (2014) 216-9.
[9] K. Fujimoto, M. Yamashita, T. Kaneko, M. Ishikawa. Influence of Bio Diesel Fuel on Engine Oil Performance. SAE Technical Paper2010.
[10] D. Shimokoji, Y. Okuyama. Analysis of Engine Oil Deterioration under Bio Diesel Fuel Use. SAE Technical Paper2009.
[11] L.E. Wagner, S.J. Clark, M.D. Schrock. Effects of soybean oil esters on the performance, lubricating oil, and water of diesel engines. SAE Technical Paper1984.

[12] A. Agarwal. Experimental investigations of the effect of biodiesel utilization on lubricating oil tribology in diesel engines. Proceedings of the Institution of Mechanical Engineers, Part D: Journal of Automobile Engineering. 219 (2005) 703-13.
[13] M. Andreae, H. Fang, K. Bhandary. Biodiesel and fuel dilution of engine oil. SAE Technical Paper2007.
[14] J. Blackburn, R. Pinchin, J. Nobre, B. Crichton, H. Cruse. Performance of lubricating oils in vegetable oil ester-fuelled diesel engines. SAE Technical Paper1983.
[15] M.J. Thornton, T.L. Alleman, J. Luecke, R.L. McCormick. Impacts of biodiesel fuel blends oil dilution on light-duty diesel engine operation. SAE Technical Paper2009.
[16] B. Gullac, O. Akalin. Frictional characteristics of IF-WS_2 nanoparticles in simulated engine conditions. Tribology Transactions. 53 (2010) 939-47.
[17] Z. Stepien, W. Urzedowska, S. Oleksiak, J. Czerwinski. Research on Emissions and Engine Lube Oil Deterioration of Diesel Engines with BioFuels (RME). SAE Technical Paper2011.
[18] S.A. Watson, V.W. Wong, D. Brownawell, S.P. Lockledge. Controlling Lubricant Acidity With an Oil Conditioning Filter. ASME 2009 Internal Combustion Engine Division Spring Technical Conference2009. pp. 749-59.
[19] S.A.G. Watson. Lubricant-derived ash: in-engine sources and opportunities for reduction. Massachusetts Institute of Technology2010.
[20] J.J. Truhan, J. Qu, P.J. Blau. The effect of lubricating oil condition on the friction and wear of piston ring and cylinder liner materials in a reciprocating bench test. Wear. 259 (2005) 1048-55.
[21] J.J. Truhan, J. Qu, P.J. Blau. A rig test to measure friction and wear of heavy duty diesel engine piston rings and cylinder liners using realistic lubricants. Tribology International. 38 (2005) 211-8.
[22] A. Agarwal, A. Dhar. Karanja oil utilization in a direct-injection engine by preheating. Part 2: experimental investigations of engine durability and lubricating oil properties. Proceedings of the Institution of Mechanical Engineers, Part D: Journal of Automobile Engineering. 224 (2010) 85-97.
[23] A. Liaquat, H. Masjuki, M. Kalam, M. Fazal, A.F. Khan, H. Fayaz, et al. Impact of palm biodiesel blend on injector deposit formation. Applied Energy. 111 (2013) 882-93.
[24] Liaquat AM, Masjuki HH, Kalam MA, R.F. IM. Impact of biodiesel blend on injector deposit formation. Energy. 72 (2014) 813-23.
[25] S.P. Lockledge, D.W. Brownawell. Materials and processes for reducing combustion by-products in a lubrication system for an internal combustion engine. Google Patents, US8607991 B2, USA, 2013.
[26] G. Sugiyama, A. Maeda, K. Nagai. Oxidation Degradation and Acid Generation in Diesel Fuel Containing 5% FAME. Training. 1999 (2007) 09-27.
[27] S.A.G.W.V.W. Wong. The Effects of Fuel Dilution with Biodiesel onLubricant Acidity, Oxidation and Corrosion –a Study with CJ-4 and CI-4 PLUS Lubricants. 2008 Diesel Engine-Efficiency and Emissions Research (DEER) Conference2008.
[28] K.R. Asfar, H. Hamed. Combustion of fuel blends. Energy Conversion and Management. 39 (1998) 1081-93.
[29] A. EPA. Comprehensive analysis of biodiesel impacts on exhaust emissions. Draft Technical Report, EPA420-02-0012002.
[30] G. Labeckas, S. Slavinskas. The effect of rapeseed oil methyl ester on direct injection Diesel engine performance and exhaust emissions. Energy Conversion and Management. 47 (2006) 1954-67.
[31] R. Mohsin, Z.A. Majid, A.H. Shihnan, N.S. Nasri, Z. Sharer. Effect of biodiesel blends on engine performance and exhaust emission for diesel dual fuel engine. Energy Conversion and Management. 88 (2014) 821-8.
[32] A. Ashraful, H. Masjuki, M. Kalam, H. Rashedul, H. Sajjad, M. Abedin. Influence of anti-corrosion additive on the performance, emission and engine component wear characteristics of an IDI diesel engine fueled with palm biodiesel. Energy Convers Manage. 87 (2014) 48-57.
[33] M. Ratoi, R.C. Castle, C.H. Bovington, H.A. Spikes. The influence of soot and dispersant on ZDDP film thickness and friction. Lubrication Science. 17 (2004) 25-43.